Hindawi
Journal of Clinical Pharmacy and Therapeutics
Volume 2024, Article ID 7008847, 14 pages
https://doi.org/10.1155/2024/7008847

Research Article

Exploring the Mechanism of Echinatin against Cervical Cancer Based on Network Pharmacology

Hu Chen and Jinlei Wang

Department of Gynecology, Shengli Oilfield Central Hospital, 31 Jinan Road, Dongying 257000, Shandong, China

Correspondence should be addressed to Jinlei Wang; 202213120153@stu.qlu.edu.cn

Received 29 October 2023; Revised 18 March 2024; Accepted 28 March 2024; Published 8 April 2024

Academic Editor: Faisal Raza

Cervical cancer significantly impacts women's health due to its high mortality rate and increasing prevalence among younger individuals, thereby posing a severe threat. Echinatin is the primary active component of licorice in traditional Chinese medicine. However, studies on its use in cervical cancer treatment are limited. In our study, 198 targets of Echinatin were identified by some databases. Among these, 40 core targets related to cervical cancer were selected. Enrichment analyses revealed that Echinatin operated through genes associated with cell cycle, apoptosis, senescence, and various cancer-related signaling pathways. Differential expression of intersecting targets was verified in the GEO database, and molecular docking also indicated a strong binding capacity between active compounds and identified targets. Moreover, the results of western blot provided further evidence at the protein level. Echinatin hindered the proliferation, migration, and invasion of HeLa and SiHa cells while increasing their apoptosis. This study predicted the potential targets and beneficial effects of Echinatin in cervical cancer treatment, which provides a new avenue for further research into the molecular mechanisms underlying the role of Echinatin in cervical cancer treatment.

1. Introduction

Cervical cancer is the most common gynecological malignancy that affects over 500,000 women and results in more than 300,000 deaths worldwide annually [1]. The global standardized incidence rate of cervical cancer is estimated to be 13.1 cases per 100,000 women [2]. High-risk human papillomavirus infection has been reported in more than 90% of cervical cancer cases [3, 4]. Clinical management of cervical cancer is challenging because of its late detection, high malignancy, poor prognosis, and lack of precise treatment options. The standard treatment currently involves surgical intervention coupled with platinum-based chemotherapy. However, this approach has not yielded satisfactory survival outcomes, and there are no specific drugs that can effectively inhibit the progression of cervical cancer [5]. Moreover, long-term radiotherapy and chemotherapy have been reported to impose heavy financial and psychological burdens on patients with cervical cancer. The estimated average economic cost of treating cervical cancer typically ranges from $368 to $11,400 [6]. It is reassuring to be aware that traditional Chinese medicine (TCM) has been effectively used for treating cancer, and its benefits are becoming increasingly evident. These advantages encompass its capability to impact signaling pathways [6], along with its cost-effectiveness and safety, resulting in minimally severe side effects.

TCM has been consistently used for over 2,000 years in China and several other countries. In TCM, licorice is considered an "essential herb" [7]. Research has found that the chemical components of licorice possess various pharmacological properties, such as anticancer, antimicrobial, anti-inflammatory, heart and liver protection, and anti-respiratory infection properties [8]. Echinatin, a biologically active flavonoid found in licorice, exhibits hepatoprotective, anti-inflammatory, and antioxidant properties [9]. In addition, Hong et al. demonstrated that Echinatin can suppress the growth and invasion of esophageal cancer tumors by inducing AKT/mTOR-dependent autophagy and apoptosis [10]. Echinatin can inhibit tumor growth and synergistically

counteract human bladder cancer cells with chemotherapy drugs by activating p38 and suppressing the Wnt/β-catenin pathway [11]. Furthermore, dual inhibition of EGFR (epithelial growth factor receptor) and MET (mesenchymal-epithelial transition factor) by Echinatin can slow cell growth and trigger apoptosis in both gefitinib-sensitive and gefitinib-resistant lung cancer cells [12]. These studies collectively demonstrate the potent antitumor capabilities of Echinatin. However, the effects of Echinatin on cervical cancer remain unknown.

Because TCM consists of intricate compounds that target multiple pathologies and pathways, the study of its mechanism is constrained by the limitations of traditional pharmacological methods. Li and Zhang proposed the concept of "network pharmacology," which provided a new method for studying the mechanisms of action of TCM [13]. Network pharmacology in TCM employs virtual computing, high-throughput data analysis, and information retrieval from network databases. It involves building biological informatics networks and analyzing their topology, focusing on the synergistic effects of multiple components, channels, and targets. Recent advancements in bioinformatics have further augmented this research methodology, enabling systematic exploration and prediction of the mechanisms underlying various diseases and drug effects.

In this study, we obtained the chemical structure of Echinatin and retrieved the major targets of cervical cancer from the gene expression omnibus (GEO) database. By taking the intersection, the common targets of Echinatin in cervical cancer were obtained. Subsequently, using the STRING platform and Cytoscape 3.7.2 software, we constructed a protein-protein interaction (PPI) network diagram. Gene ontology (GO) and Kyoto Encyclopedia of genes and genomes (KEGG) enrichment analyses were conducted using the DAVID database, and an "Echinatin–intersection target-pathway-cervical cancer" network diagram was created. Subsequently, we performed molecular docking of the filtered protein with Echinatin and experimentally verified the expression of related proteins in SiHa cells after Echinatin treatment. After conducting multiple experiments, it was eventually proven that Echinatin effectively regulates the proliferation, migration, invasion, and apoptosis of cervical cancer cells (HeLa and SiHa). These findings provide crucial insights into the mechanisms by which Echinatin treats cervical cancer (Figure 1).

2. Materials and Methods

2.1. Echinatin Target Prediction. First, the chemical structure of Echinatin was downloaded from the PubChem database (https://pubchem.ncbi.nlm.nih.gov) [14]. Second, the target was predicted using the SwissTargetPrediction (https://www.swisstargetprediction.ch/) [15], SuperPred (https://prediction.charite.de/subpages/target_prediction.php) [16], and SEA (https://sea.bkslab.org/) [17] databases. Third, the names were standardized using the UniProt database (https://www.uniprot.org.hnucm.opac.vip/). Finally, non-human targets were eliminated, and data were consolidated by merging and removing duplicates to determine the target of Echinatin.

2.2. Predictive Target Genes for Cervical Cancer. The GSE89657 (14 cancers and 4 normals) dataset was downloaded from the gene expression omnibus (GEO) database (https://www.ncbi.nlm.nih.gov/geo/) [18].

GSE29570 (45 cancers and 17 normals) and GSE63678 (17 cancers and 18 normals) serve as validation cohorts. Differential analysis on this chip was performed using R software. Differential genes were selected as disease targets based on the criteria of $P < 0.05$ and $|\log2 \text{ fold change (FoldChange)}| \geq 1$.

2.3. Identifying the Intersecting Targets of Echinatin and Cervical Cancer. The intersection of the targets of Echinatin and disease targets of cervical cancer was determined using the online platform Venny 2.1 (https://bioinfogp.cnb.csic.es/tools/venny/).

2.4. PPI Analysis and Core Target Screening. The intersection targets in the STRING database (https://string-db.org) [19] were analyzed, and the biological species was set as "*Homo sapiens*," with a minimum required interaction score of 0.4. The unconnected nodes were hidden in the network while the PPI network was constructed. Subsequently, Cytoscape 3.7.2 software was used for visual analysis of the PPI network.

2.5. GO and KEGG Analyses. The intersected targets were imported into the DAVID database (https://david.ncifcrf.gov/summary.jsp) [20] for GO and KEGG analyses. The P value of <0.05 was considered statistically significant.

2.6. Molecular Docking. Core targets were docked with Echinatin using molecular docking techniques. The sdf file of the core target structure was downloaded from the Protein Data Bank (PDB) database (https://www.rcsb.org.hnucm.opac.vip/). The sdf file of Echinatin was downloaded from the PubChem database (https://pubchem.ncbi.nlm.nih.gov). Online molecular docking was performed on the CB-DOCK2 database (https://cadd.labshare.cn.hnucm.opac.vip/cb-dock2/php/index.php) [21]. Each receptor-ligand pair was docked six times, and the lowest binding energy was recorded. The optimal binding conformation was selected for interaction analysis, and a protein-ligand interaction diagram was generated.

2.7. Cell Culture. HeLa and SiHa cells were cultured under specific conditions using materials obtained from the American Type Culture Collection (ATCC). Cells were grown in Dulbecco's Modified Eagle Medium (Gibco, USA) with 10% fetal bovine serum (Gibco, USA) at 37°C and 5% carbon dioxide. Echinatin (PHL83847) was obtained from Sigma-Aldrich (CAS: 34221-41-5, USA). Echinatin treatments of cervical cancer cells were performed at final concentrations of 10, 20, and 40 μM for 48 h. Cells in the control group were only treated with an equal volume of phosphate-buffered saline (PBS).

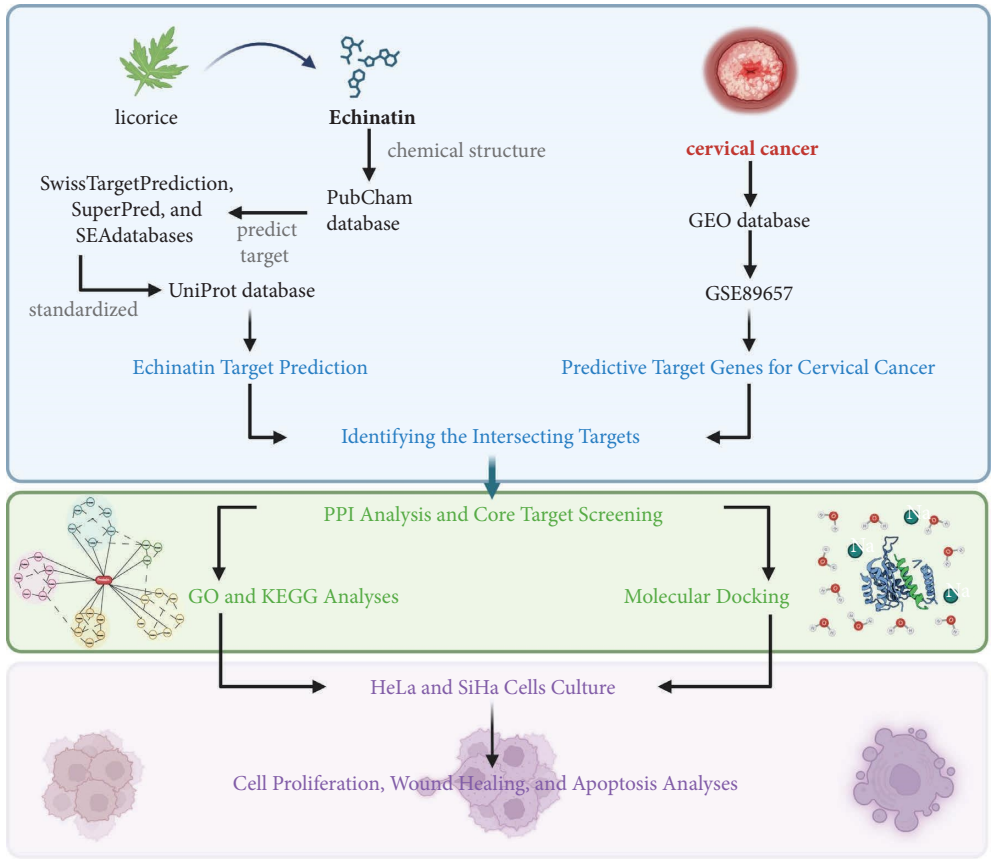

Figure 1: Road map of the main research ideas in this article.

2.8. Cell Counting Kit-8 (CCK-8 Assay). In this experiment, we use high sensitivity cell counting kit (Beyotime, China) to detect the quantity of 10^5 (100 μl) cells per well and 10 μl of drugs per well. The control group was 100 μl quantitative cells +10 μl PBS. The survival rate of the cells is expressed by T/C, where T is the OD value of the added cells and C is the OD value of the control cells.

2.9. Western Blot Assay. Total protein was obtained from cells using RIPA lysis buffer (Solarbio, China). Protein concentration was then assessed using the BCA Protein Assay Kit (Beyotime, China). Proteins from different samples were separated via sodium dodecyl sulfate–polyacrylamide gel electrophoresis and transferred onto a polyvinylidene difluoride membrane (Beyotime, China). The membrane was then sealed with 5% bovine serum albumin (Solarbio, China) at room temperature (RT, 26°C) for 1.5 h. Subsequently, it was incubated with different primary antibodies (1 : 1,000–2,000) overnight at 4°C. After removing unbound primary antibodies from the membrane, it was incubated with corresponding enzyme-labeled secondary antibodies (1 : 5,000–8,000) at RT for 1 h. Finally, the film was analyzed for grayscale values of the bands using the ECL Detection Kit (P0018S; Beyotime) and image processing software Image J.

2.10. Flow Cytometric Analysis of Cell Apoptosis. The cells were counted at an appropriate quantity and cultured in a six-well plate overnight. Here, cells were treated with Echinatin at final concentrations of 10, 20, and 40 μM for 48 h. Cell apoptosis was detected using the Annexin V-FITC/PI Apoptosis Detection Kit (A211-01; Vazyme, China). Approximately 1×10^6 cells were mixed with a mixture of Annexin V-FITC and PI, followed by incubation at RT in the dark for 15 min. Finally, cell distribution was analyzed using a FACScalibur flow cytometer (BD Biosciences, USA), and data were analyzed using Flow Jo software.

2.11. Wound Healing Assay. The cells were placed in a six-well plate and allowed to grow for 24 h until they reached 90%–100% confluency. A pipette tip was used to make scratches on each well of the six-well plate. Next, the movement of the cells was examined under a microscope, and images were captured at different time intervals (0 and 24 h).

2.12. Cell Proliferation Ability Detection. EdU and clonogenic assays were used to detect the proliferation of cervical cancer cells. The specific operations for the EdU assay were as follows. According to the experimental plan of the user manual, the BeyoClick EdU-488 Cell Proliferation Assay Kit (C0071S;

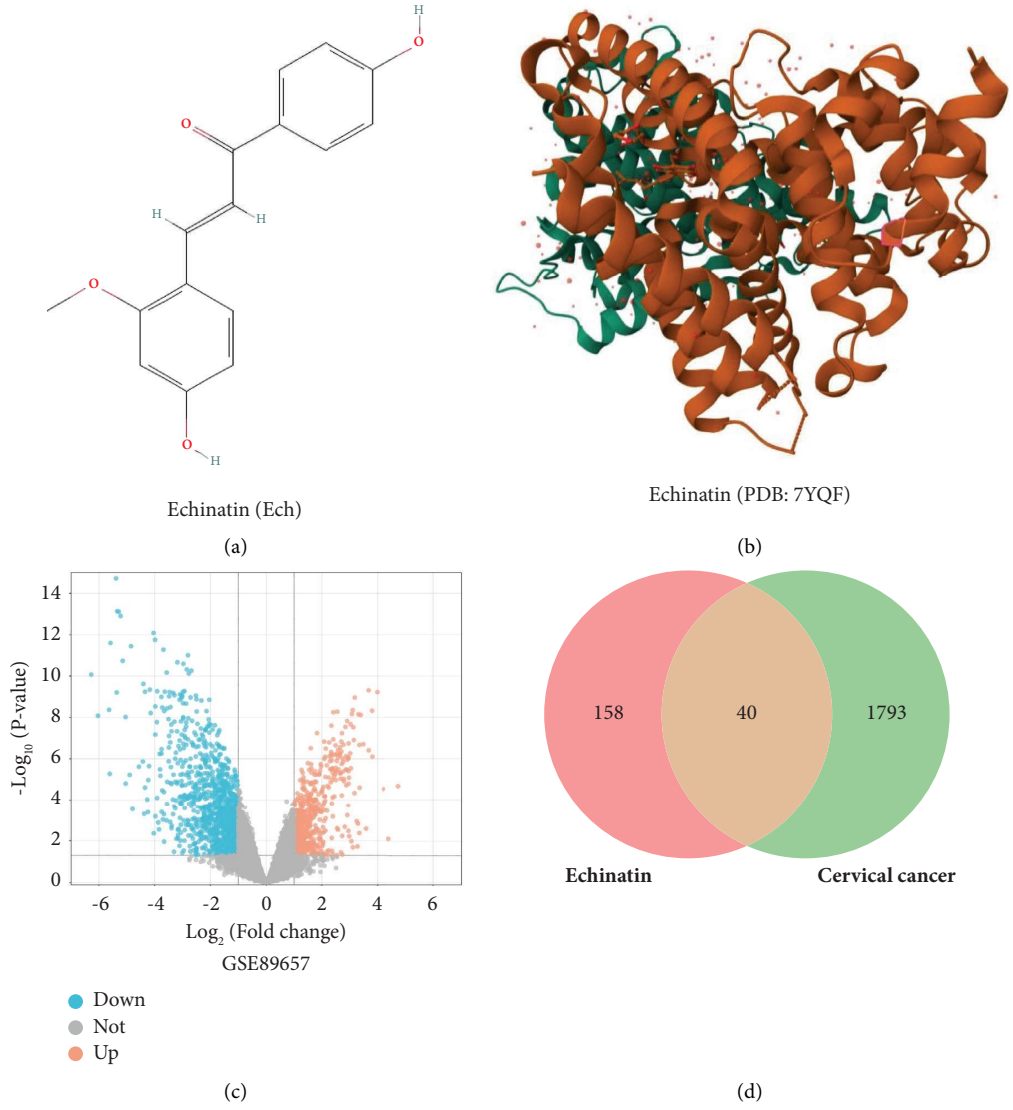

FIGURE 2: Determination of intersection targets between Echinatin and cervical cancer. (a) Chemical structure of Echinatin. (b) Three-dimensional structure of Echinatin. (c) Disease targets of cervical cancer. (d) Intersection target of Echinatin and cervical cancer.

Beyotime) was used to detect cell proliferation. Cells were observed under a fluorescence microscope and imaged. Proliferating cells exhibited bright green fluorescence. The specific procedure for the clonogenic assay was as follows. After the cells were treated with Echinatin for 48 h, they were fixed in 4% paraformaldehyde for 10 min and stained with crystal violet (0.1% w/v) for 15 min. Excess dye was washed with PBS, and images were captured using an inverted fluorescence microscope (Observer 7; Carl Zeiss, Germany).

2.13. Statistical Analysis. All analyses were conducted using GraphPad Prism 9.0 software. Data are presented as mean ± standard error (SEM, $n \geq 3$). Nonparametric t-tests were used to compare the two groups. One-way analysis of variance and Tukey's test were used to evaluate and determine statistical differences among multiple groups. P value of <0.05 was considered statistically significant.

3. Results

3.1. Determination of Intersection Targets between Echinatin and Cervical Cancer. First, the chemical structure and three-dimensional structure of Echinatin were retrieved from the PubChem and PDB databases (Figures 2(a) and 2(b)). Potential target sites were then predicted using three different databases: SwissTargetPrediction, SuperPred, and SEA, which yielded 81, 88, and 58 potential targets, respectively. These results were standardized and merged by removing duplicates, which resulted in 198 target sites for Echinatin. Second, we searched "Cervical cancer" as a keyword in the GEO database, leading to the acquisition of the gene chip GSE89657. We selected differential genes as cancer targets based on the conditions of $P < 0.05$ and $|\log2FC| \geq 1$. In total, 1,833 differentially expressed genes were identified, including 1,213 downregulated and 620 upregulated genes (Figure 2(c)). Finally, we intersected the targets of Echinatin

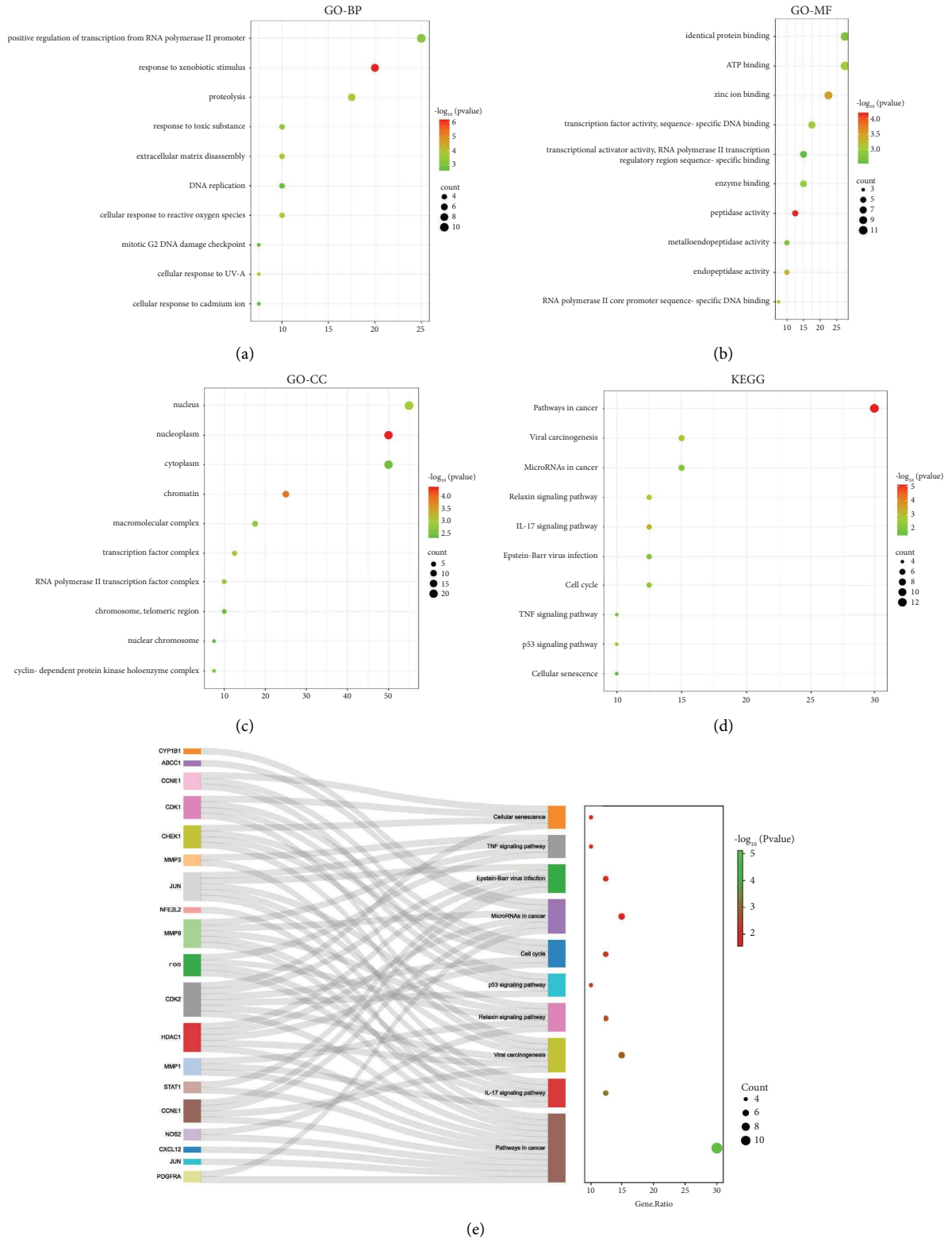

FIGURE 3: Gene ontology (GO) and kyoto encyclopedia of genes and genomes (KEGG) analyses of cross-targeted genes. (a–c) GO analysis of Echinatin and cervical cancer cross-target genes. The ontology covers three domains: biological process (BP), cellular component (CC), and molecular function (MF). *Note*. Only the top 10 entries are shown in the figure. (d) KEGG analysis of cross-target genes between Echinatin and cervical cancer. (e) Cross-summary of the enrichment results of the KEGG pathways and literature screening of items related to cervical cancer.

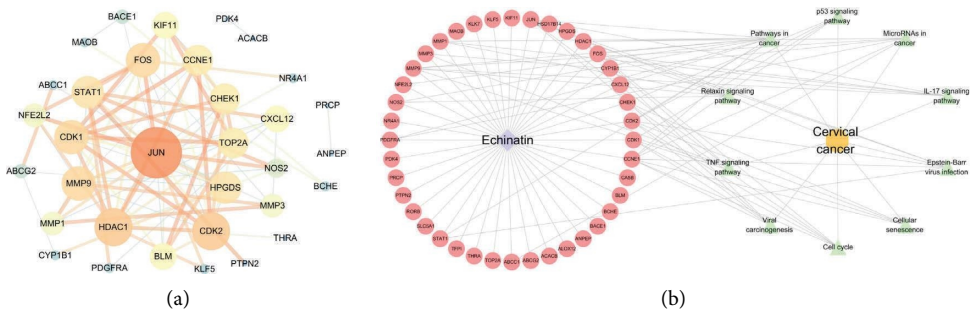

(a) (b)

FIGURE 4: Network construction between Echinatin and cervical cancer. (a) Protein–protein interaction analysis and core target selection for proteins. (b) Echinatin–overlapping target–pathway network map of cervical cancer.

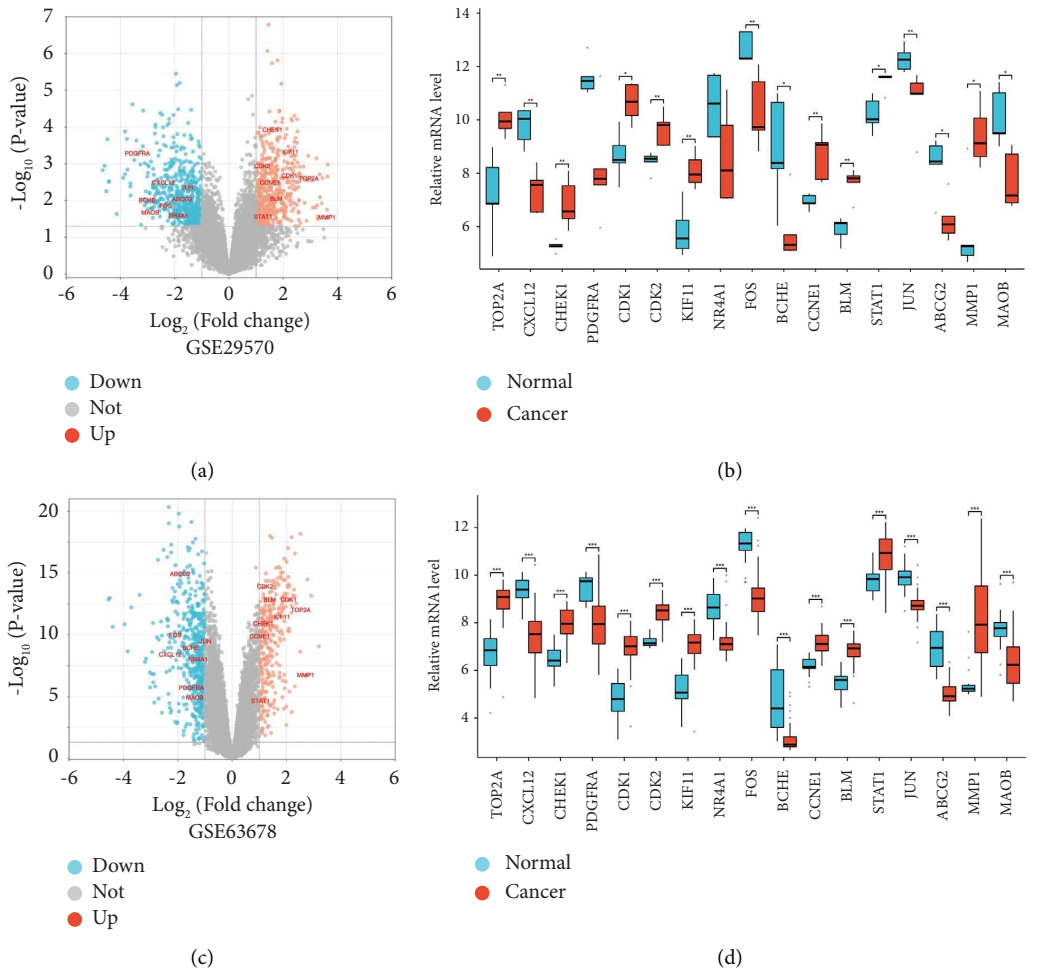

FIGURE 5: Gene expression omnibus database verification of intersection targets. (a) Volcano diagram showing the differentially expressed genes (DEGs) with |log2 fold change (FC)| > 1 and $P < 0.05$ based on the GSE29570 dataset. (b) Cross-target genes of differential analysis in the GSE29570 dataset. (c) Volcano diagram showing the DEGs with |log2FC| > 1 and $P < 0.05$ based on the GSE63678 dataset. (d) Cross-target genes of differential analysis in the GSE63678 dataset. $^{*}P < 0.05$, $^{**}P < 0.01$, and $^{***}P < 0.001$.

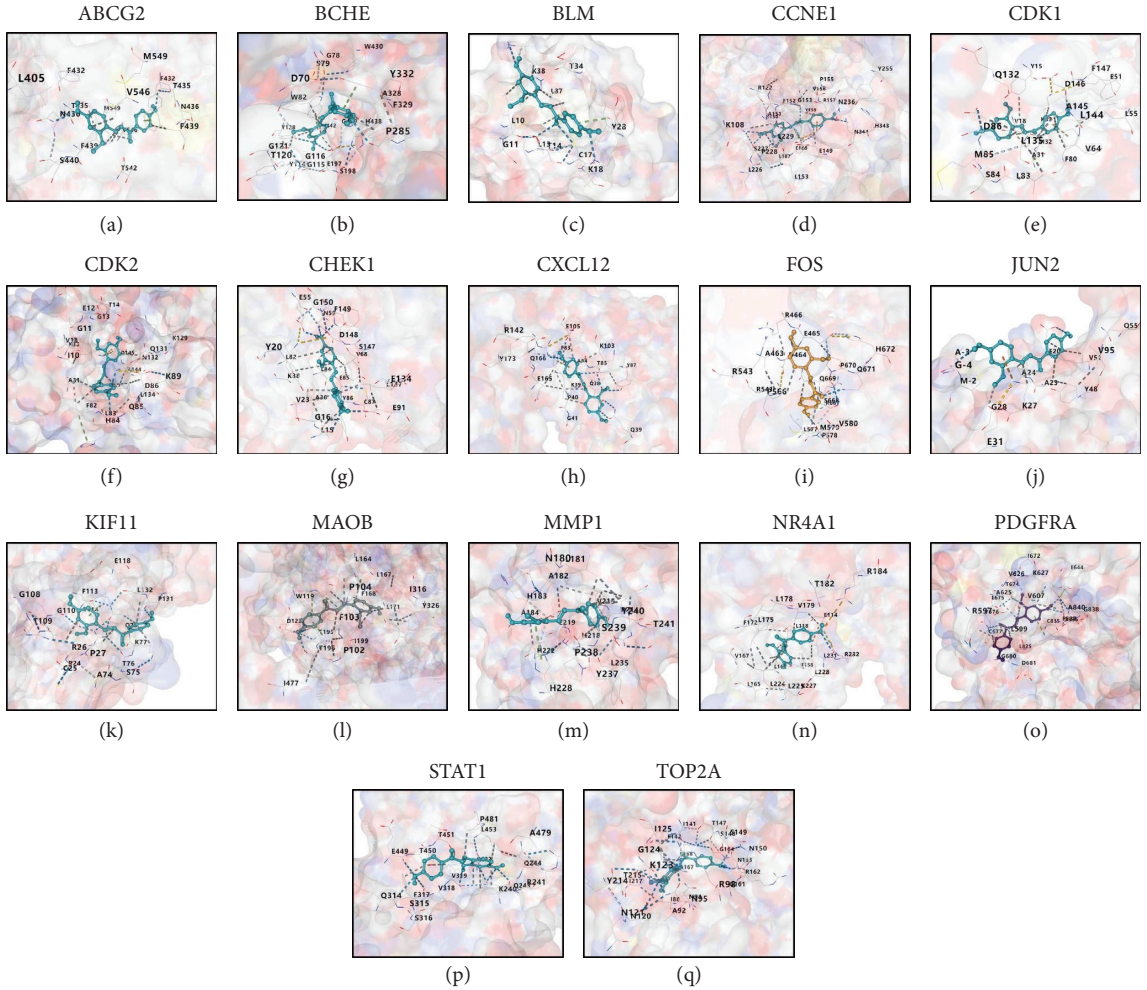

Figure 6: Molecular docking between cross-targets and Echinatin. (a–q) Echinatin and (a) ABGC2. (b) BCHE. (c) BLM. (d) CCNE1. (e) CDK1. (f) CDK2. (g) CHEK1. (h) CXCL12. (i) FOS. (j) JUN2. (k) KIF11. (l) MAOB. (m) MMP1. (n) NR4A1. (o) PDGFRA. (p) STAT1. (q) TOP2A docking result graph. Echinatin is represented as a light-colored cartoon model, and the ligand is shown as a stick model, with their binding sites labeled in the figure. Nonpolar hydrogen atoms are omitted. Hydrogen bonding, ion interactions, and hydrophobic interactions are depicted as yellow, magenta, and green dashed lines, respectively.

with the tumor target genes of cervical cancer using the Venny 2.1 online platform [22], obtaining 40 intersecting target points (Figure 2(d)).

3.2. GO and KEGG Enrichment Analyses of Cross-Targeted Genes. To deepen our understanding of the cross-target genes of Echinatin and cervical cancer, we conducted a GO analysis encompassing biological processes (BPs), cellular components (CCs), and molecular functions (MFs) (Figures 3(a)–3(c)). In the BP group, the active targets were predominantly related to the "positive regulation of transcriptional from ribonucleic acid (RNA) polymerase II promoter," "extracellular matrix degradation," "cell response to metal ions," "cell response to external stimuli," "cell response to toxic substances," and "cell response to reactive oxygen species" (Figure 3(a)). In the CC group, genes were mainly enriched in areas such as the "nucleus," "nucleoplasm," "cytoplasm," "chromatin," "cyclin-dependent protein kinase holoenzyme complex," and "RNA polymerase II transcription factor complex" (Figure 3(c)). In the MF group, enrichment was observed in functions such as "identical protein binding," "ATP binding," "activated transcription factor binding," "zinc ion binding," "transcription factor activity, sequence-specific deoxyribonucleic acid (DNA) binding," "transcription activator activity, RNA polymerase II transcription regulatory region sequence-specific binding," "enzyme binding," and "peptidase activity" (Figure 3(b)).

Furthermore, we correlated the KEGG pathway enrichment analysis results with extensive literature research, categorizing the potential impact of different genes on cervical cancer (Figure 3(e)). This analysis provides valuable insights for future research into the cross-target genes of Echinatin and cervical cancer, particularly their roles in various pathways during disease onset and progression.

The KEGG analysis focused on identifying the primary effects of Echinatin. As shown in Figure 3(d), the cross-gene of Echinatin with cervical cancer was primarily associated with the pathways involved in cancer development as well as

Table 1: Binding energy of the complex formed by small-molecule protein and Echinatin.

Molecular	Binging energy (kcal/mol)
TOP2A	−8.6
CXCL12	−6.8
CHEK1	−8.8
PDGFRA	−9.2
CDK1	−8.1
CDK2	−7.7
KIF11	−7.7
NR4A1	−7.7
Fos	−7.1
BCHE	−8.9
CCNE1	−8.7
BLM	−5.8
STAT1	−7.4
JUN	−5.9
ABCG2	−8.4
MMPI	−7.5
MAOB	−9.9

Note. The binding energy of the complex formed by small-molecule protein and Echinatin. The unit is kcal/mol, and the docking results are considered reliable if they are less than −1.2 kcal/mol.

microRNAs, cell cycle, tumor necrosis factor signaling pathway, p53 signaling pathway, interleukin-17 signaling pathway, relaxin signaling pathway, Epstein–Barr virus infection, cell aging, and other processes (Figure 3(d)). In addition, we correlated the KEGG pathway enrichment analysis results with extensive literature research and categorized the potential impact of different genes on cervical cancer (Figure 3(e)). This analysis provides valuable insights for future research into the cross-target genes of Echinatin and cervical cancer, particularly their roles in various pathways during disease onset and progression.

3.3. Network Construction between Echinatin and Cervical Cancer. After retrieving the relationship information between Echinatin and cervical cancer target genes from the STRING website, we constructed a gene-gene interaction network. This network comprised 33 nodes and 89 edges, as shown in Figure 4(a). Within the PPI network, the core genes identified with higher degree values included *JUN*, *CXCL12*, *PDGFRA*, *NR4A1*, *FOS*, *BCHE*, *ABCG2*, *MAOB*, *TOP2A*, *CHEK1*, *CDK1*, *CDK2*, *KIF11*, *CCNE1*, *BLM*, *STAT1*, and *MMP1* (Figure 4(a)). Subsequently, we used Cytoscape 3.7.2 software [23] to visualize the interconnections among Echinatin, intersecting targets, pathways, and cervical cancer. This process led to the construction of the Echinatin-intersecting target-pathway-cervical cancer network, as shown in Figure 4(b).

3.4. GEO Database Verification of Intersection Targets. In the GEO database, using "cervical cancer" as the keyword, datasets that met the criteria were selected to validate the intersection targets. Using data obtained from the GSE29570 and GSE63678 datasets, we analyzed the differential expression of cross-target genes. As shown in Figure 4, in the cervical cancer group, the expression of *TOP2A*, *CHEK1*, *CDK1*, *CDK2*, *KIF11*, *CCNE1*, *BLM*, *STAT1*, and *MMP1* was upregulated compared with that of the control group, whereas the expression of *CXCL12*, *PDGFRA*, *NR4A1*, *FOS*, *BCHE*, *JUN*, *ABCG2*, and *MAOB* was downregulated (Figures 5(a)–5(d)).

3.5. Molecular Docking between Cross-Targets and Echinatin. To validate the effective binding of Echinatin with small-molecule ligands encoded by the selected cross-target genes in cervical cancer, molecular docking experiments were performed. The crystal structure of Echinatin (PDB: 7YQF) was obtained from the PDB [24]. The protonation state of the small molecule was set to a pH level of 7.4, and Open Babel was used to expand the compound into a three-dimensional structure. Receptor proteins and ligands were prepared using the AutoDock tool (ADT3). The docking box was created using the AutoGrid program, followed by molecular docking using Autodock Vina (1.2.0). The protein-ligand interaction results visualized using PyMOL are shown in Figure 6. Subsequent analysis of molecular docking results with Discovery Studio revealed that the small-molecule proteins encoded by MAOB (−9.9 kcal/mol), PDGFRA (−9.2 kcal/mol), BCHE (−8.9 kcal/mol), CHEK1 (−8.8 kcal/mol), and CCNE1 (−8.7 kcal/mol) had a lower binding energy with Echinatin (Table 1). These binding positions were more suitable and resulted in the formation of more stable chemical bonds, thereby indicating a better binding effect.

3.6. Impact of Echinatin on the Expression of Proteins Related to Cervical Cancer Cells. Then, we investigated the impact of Echinatin on cervical cancer cells by conducting in vitro experiments. We discovered that after 24 and 48 hours of treatment, 10 μm of Echinatin significantly affected cell proliferation, with a more pronounced effect observed at 48 hours (Supplementary Figure 1a). Additionally, at 48 hours, Echinatin doses of 10 μm, 20 μm, and 40 μm were found to have a significant impact on cell proliferation (Supplementary Figure 1b). Western blot analysis was conducted to detect changes in the five corresponding key proteins in HeLa cells under different Echinatin concentrations (10, 20, and 40 μM). As depicted in Figure 7, compared with the PBS group, the Echinatin-treated group exhibited significant downregulation of the expression of *CDK1*, *CDK2*, *CCNE1*, *MAOB*, and *CHEK1* in HeLa cells. The most noticeable effect was observed at the 40 μM concentration of Echinatin (Figures 7(a)–7(f)). The aforementioned five proteins, which play a crucial role in the onset and progression of tumors, are pivotal in regulating the cell cycle and DNA damage repair processes in eukaryotic cells. They are also intimately linked to tumor cell proliferation, differentiation, migration, and invasion.

3.7. Inhibitory Effect of Echinatin on Cervical Cancer. Building on the observed downregulation of the expression of *CDK1*, *CDK2*, *CCNE1*, *MAOB*, and *CHEK1* in HeLa cells by Echinatin, we hypothesized that Echinatin could affect the proliferation, migration, invasion, and apoptosis of cervical cancer cells. Therefore, we conducted further

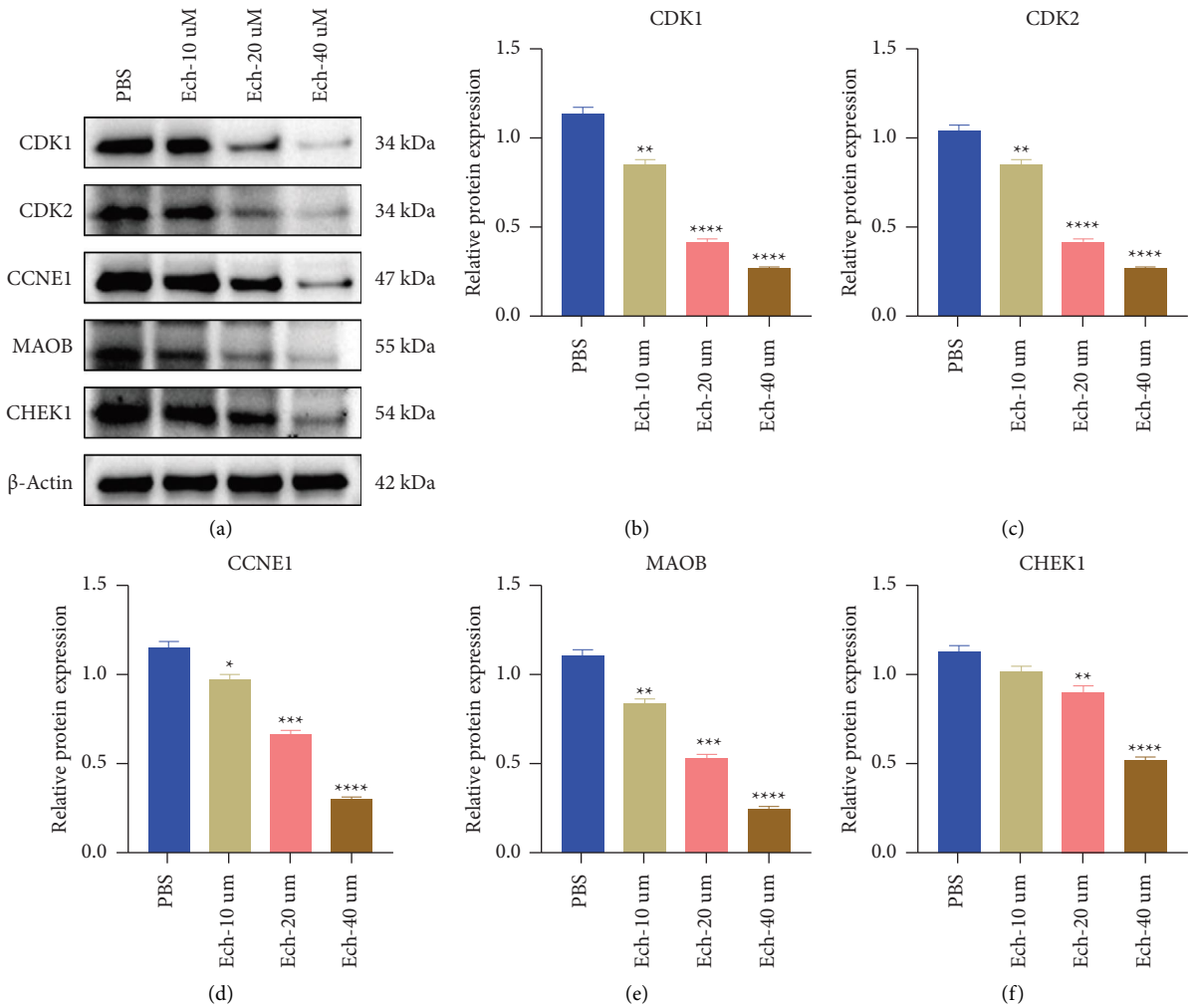

Figure 7: Impact of Echinatin on the expression of proteins related to cervical cancer cells. (a) Western blotting detects the protein expression levels of CDK1, CDK2, CCNE1, MAOB, and CHEK1, which are closely associated with the occurrence and development of cervical cancer cells in HeLa. B-actin is used as an internal control. (b–f) The aforementioned five proteins are shown in a bar chart separately for their relative expression levels compared with β-actin in the samples. $^{*}P < 0.05$, $^{**}P < 0.01$, $^{***}P < 0.001$, and $^{****}P < 0.0001$.

experiments. Compared with the control group, Echinatin treatment significantly reduced the proliferation of cervical cancer cells (HeLa and SiHa), with a more notable effect in HeLa cells (Figures 8(a) and 8(b)). In addition, transwell invasion assay and wound healing assay showed that Echinatin markedly decreased the invasive and migration capabilities of cervical cancer cells (Figures 8(c) and 8(d)). These findings suggest that Echinatin can inhibit the proliferation, migration, and invasion of cervical cancer cells, thereby potentially hindering the progression and development of cervical cancer.

3.8. Echinatin Promotes Cervical Cancer Cell Apoptosis. A previous study suggested that inhibiting CDK1 and CDK2 can not only suppress tumor cell proliferation but also enhance tumor cell apoptosis in human tumors [25]. Our previous results showed that Echinatin significantly reduces the expression of CDK1 and CDK2 in cervical cancer cells. Consequently, we hypothesized that Echinatin influences the apoptosis of these cells. Flow cytometry results confirmed that Echinatin promotes apoptosis in HeLa and SiHa cells in a dose-dependent manner, with the most effective apoptosis promotion observed at a concentration of 40 μM (Figure 9(a)).

In addition, we evaluated the expression levels of apoptosis-related proteins in cervical cancer cells after Echinatin treatment. The results revealed a significant decrease in the expression of the antiapoptotic protein Bcl-2 and an enhanced expression of the proapoptotic proteins BAX and cleaved caspase-3 (c-caspase-3) following Echinatin treatment (Figure 9(b)). These findings indicated that Echinatin enhances its antitumor activity by promoting apoptosis in cervical cancer cells.

4. Discussion

Echinatin, a natural compound derived from the Chinese herb licorice, is known for its hepatoprotective, anti-inflammatory, and antioxidant properties [9]. Previous studies have shown its therapeutic effects on various cancers,

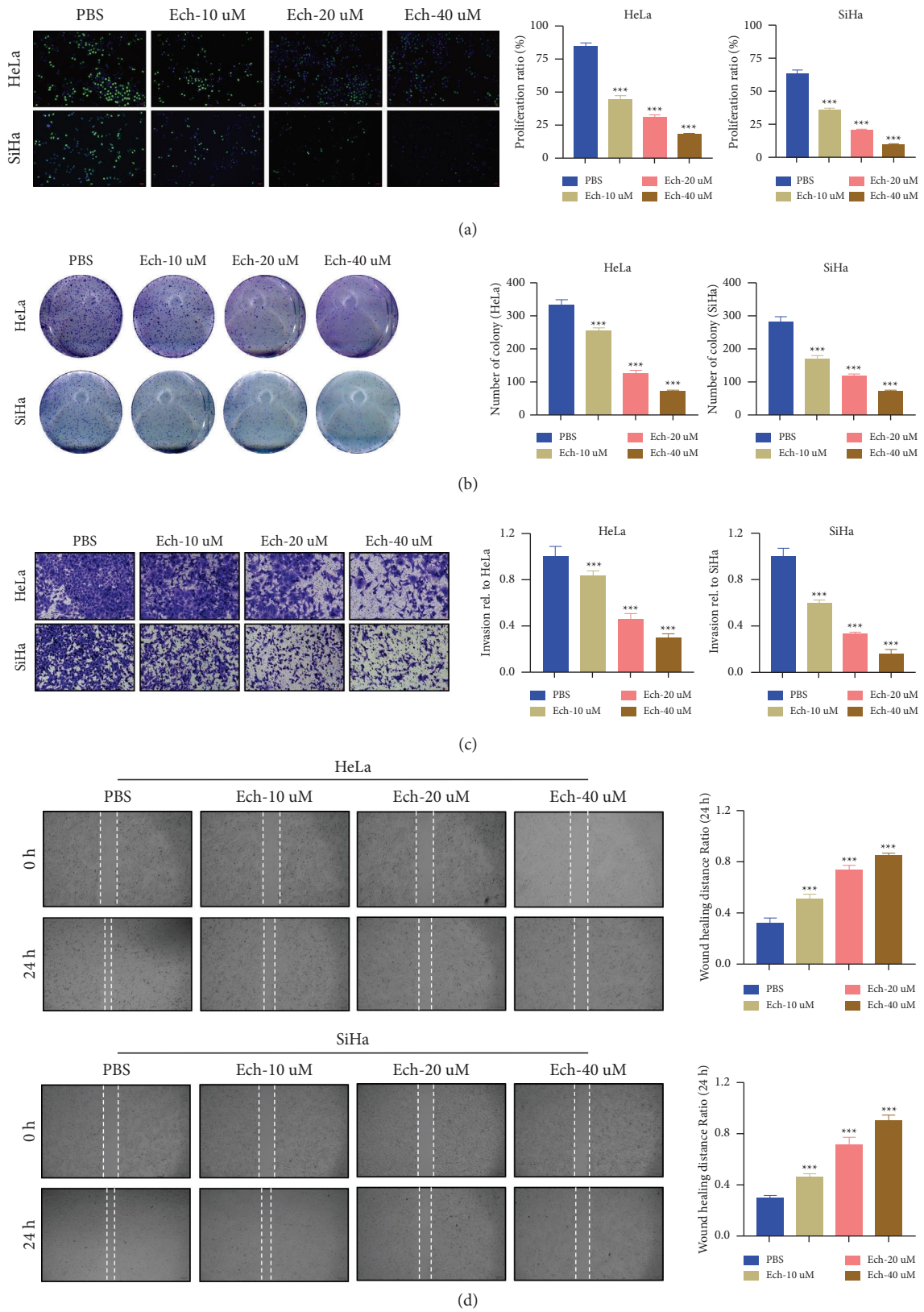

Figure 8: Inhibitory effect of Echinatin on cervical cancer. (a) The EdU assay detects the proliferation of cervical cancer cells HeLa and SiHa. (b) The clonogenic assay detects the proliferation of HeLa and SiHa. (c) The transwell invasion assay detects the invasive abilities of cervical cancer cells HeLa and SiHa. (d) The wound healing assay detects the migration ability of cervical cancer cells HeLa and SiHa. *** $P < 0.001$.

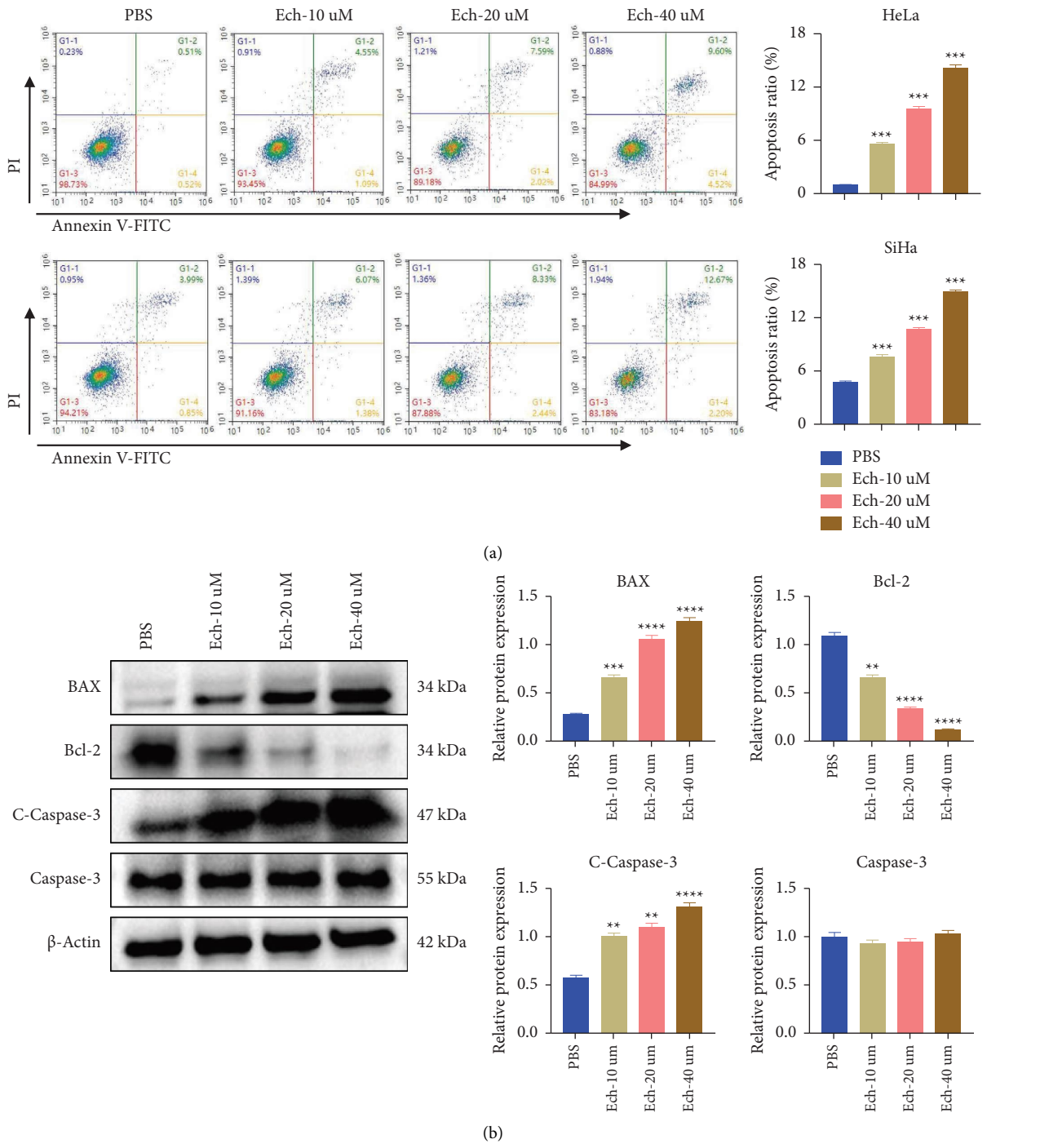

Figure 9: Echinatin promotes cervical cancer cell apoptosis. (a) Different concentrations of Echinatin are used to assess apoptosis in HeLa and SiHa cervical cancer cells. (b) The expression levels of apoptotic-related proteins in HeLa and SiHa. The quantitative relative expression levels of apoptosis-related proteins are shown in the right figure. $^{**}P < 0.01$, $^{***}P < 0.001$, and $^{****}P < 0.0001$.

including lung cancer [12], esophageal cancer [10], bladder cancer [11], colorectal cancer [26], and osteosarcoma [27]. Although cervical cancer is a prevalent gynecological malignancy [28], no studies have investigated the effect of Echinatin on cervical cancer. This study explores the potential impact of Echinatin on cervical cancer through a combination of network pharmacology and experimental approaches, aiming to provide a foundation for future research.

Initially, we acquired the chemical structure of Echinatin through retrieval and predicted its targets using the SwissTargetPrediction, SuperPred, and SEA databases. Using the GEO database, we identified 40 intersecting targets related to cervical cancer. By constructing molecular system-level compound–protein interaction networks, we could effectively screen these core targets. The intersection targets underwent GO and KEGG analyses using the DAVID

database, with the top 10 entries in each category being highlighted. Molecular docking was employed to assess the interaction of Echinatin with potential targets. This process identified five tumor-related proteins: CDK1, CDK2, CCNE1, MAOB, and CHEK1.

HeLa and SiHa cervical cancer cells were used for western blot analysis of these five proteins. We found that Echinatin significantly inhibited their expression and showed a dose-dependent effect. Finally, through experiments such as EdU assay, colony formation assay, transwell invasion assay, wound healing assay, and flow cytometry, we independently demonstrated that Echinatin inhibits the proliferation, invasion, and migration of HeLa and SiHa cells and promotes tumor cell apoptosis, showing a good anticancer effect in cervical cancer.

Cell cycle dysregulation is a hallmark of human cancer [29]. Cyclin-dependent kinases (CDKs) and cyclins are crucial for cell cycle regulation. Studies have shown that CDK1 and CDK2 are key in regulating DNA synthesis, G1/S phase transition, and G2 progression in tumor cells, thus facilitating cancer-related processes such as proliferation, survival, and epithelial-mesenchymal transition [30–32]. Cyclin E1 (CCNE1), which is vital for cell cycle regulation, promotes the G1 to S phase transition by activating CDK2, thereby initiating DNA replication [33]. MAOB plays a significant role in the structural modification of chromosomes and the regulation of gene expression. Its overexpression in cancer cells leads to increased deacetylation, resulting in tighter DNA and histone interactions and nucleosome compaction, which is unfavorable for the expression of specific genes, including some tumor suppressor genes [34, 35]. Numerous studies have shown that the expression level of MAOB is closely associated with tumor differentiation, lymph node metastasis, and patient survival prognosis [35–37]. Checkpoint kinase 1 (CHEK1), a member of the CHEK family, is a serine/threonine-specific protein kinase that mediates cell cycle arrest in response to DNA damage [38], which is closely associated with the occurrence and development of tumors [38–40]. However, the role of these five proteins in cancer treatment with Echinatin remains under-explored. Our network pharmacology and experimental studies suggest that Echinatin can serve as a therapeutic agent in inhibiting cervical cancer by targeting these five tumor-associated genes.

This study broadens our understanding of the potential role of Echinatin in treating cervical cancer and contributes to our knowledge of TCM application in cancer therapy. Despite these advancements, this study has certain limitations. First, a more comprehensive collection of TCM-specific target genes is required to enhance the reliability of network pharmacology analysis results. Second, our research is limited to cellular studies, necessitating further validation of these findings through animal experiments. Moreover, it is crucial to explore how these five genes respond to Echinatin as a standalone treatment versus its combination with other anticancer drugs.

5. Conclusions

In summary, network pharmacology analysis suggested that Echinatin targets multiple aspects of cervical cancer. It primarily inhibits the proliferation, migration, and invasion of cervical cancer cells by downregulating the protein levels of CDK1, CDK2, CCNE1, MAOB, and CHEK1 and concurrently promotes apoptosis, thereby exhibiting its antitumor properties. Our findings indicate that Echinatin holds promise as a potential new therapeutic option for cervical cancer treatment.

Abbreviations

TCM:	Traditional Chinese medicine
PPI:	Protein-protein interaction
GO:	Gene ontology
KEGG:	Kyoto encyclopedia of genes and genomes
PDB:	Protein data bank
RT:	Room temperature
PI:	Propidium iodide
BP:	Biological processes
CC:	Cellular components
MF:	Molecular functions
ADT:	AutoDock tool
C-Caspase 3:	Cleaved caspase-3
CCK-8:	Cell counting kit-8.

Data Availability

All data are provided in this study, and raw data can be requested to the corresponding author.

Ethical Approval

The authors are accountable for all aspects of the work in ensuring that questions related to the accuracy or integrity of any part of the work are appropriately investigated and resolved. This study was approved by Shengli Oilfield Central Hospital.

Conflicts of Interest

The authors declare that the research was conducted in the absence of any commercial or financial relationships that could be construed as a potential conflicts of interest.

Authors' Contributions

Hu Chen and Jinlei Wang were responsible for conception and design. Hu Chen analyzed and interpreted the study. Hu Chen was responsible for data collection. Hu Chen and Jinlei Wang wrote the article. Hu Chen critically revised the study. Jinlei Wang performed statistical analysis. Jinlei Wang took the overall responsibility. All authors read and approved the final manuscript.

Supplementary Materials

Supplementary Figure 1: CCK-8 testing was performed to investigate the inhibitory effect of Echinatin on cervical cancer cells. (*Supplementary Materials*)

References

[1] R. B. Perkins, N. Wentzensen, R. S. Guido, and M. Schiffman, "Cervical cancer screening: a review," *JAMA*, vol. 330, no. 6, p. 547, 2023.

[2] S. Bewley, "HPV vaccination and cervical cancer screening," *The Lancet*, vol. 399, no. 10339, p. 1939, 2022.

[3] P. Piña-Sánchez, "Human papillomavirus: challenges and opportunities for the control of cervical cancer," *Archives of Medical Research*, vol. 53, no. 8, pp. 753–769, 2022.

[4] P. Olusola, H. N. Banerjee, J. V. Philley, and S. Dasgupta, "Human papilloma virus-associated cervical cancer and health disparities," *Cells*, vol. 8, no. 6, p. 622, 2019.

[5] M. D. A. Paskeh, S. Mirzaei, M. H. Gholami et al., "Cervical cancer progression is regulated by SOX transcription factors: revealing signaling networks and therapeutic strategies," *Biomedicine & Pharmacotherapy*, vol. 144, Article ID 112335, 2021.

[6] S. Wilailak, M. Kengsakul, and S. Kehoe, "Worldwide initiatives to eliminate cervical cancer," *International Journal of Gynecology & Obstetrics*, vol. 155, no. 1, pp. 102–106, 2021.

[7] Y. Ding, E. Brand, W. Wang, and Z. Zhao, "Licorice: resources, applications in ancient and modern times," *Journal of Ethnopharmacology*, vol. 298, Article ID 115594, 2022.

[8] M. Jiang, S. Zhao, S. Yang et al., "An "essential herbal medicine"—licorice: A review of phytochemicals and its effects in combination preparations," *Journal of Ethnopharmacology*, vol. 249, Article ID 112439, 2020.

[9] Y. Fu, J. Chen, Y.-J. Li, Y.-F. Zheng, and P. Li, "Antioxidant and anti-inflammatory activities of six flavonoids separated from licorice," *Food Chemistry*, vol. 141, no. 2, pp. 1063–1071, 2013.

[10] P. Hong, Q.-W. Liu, Y. Xie et al., "Echinatin suppresses esophageal cancer tumor growth and invasion through inducing AKT/mTOR-Dependent autophagy and apoptosis," *Cell Death & Disease*, vol. 11, no. 7, p. 524, 2020.

[11] X. Wang, L. Luo, J. Xu et al., "Echinatin inhibits tumor growth and synergizes with chemotherapeutic agents against human bladder cancer cells by activating p38 and suppressing Wnt/β-catenin pathways," *Genes & Diseases*, vol. 11, no. 2, pp. 1050–1065, 2024.

[12] H. Oh, M. Lee, E. Kim et al., "Dual inhibition of EGFR and MET by Echinatin retards cell growth and induces apoptosis of lung cancer cells sensitive or resistant to gefitinib," *Phytotherapy Research*, vol. 34, no. 2, pp. 388–400, 2020.

[13] S. Li and B. Zhang, "Traditional Chinese medicine network pharmacology: theory, methodology and application," *Chinese Journal of Natural Medicines*, vol. 11, no. 2, pp. 110–120, 2013.

[14] S. Kim, J. Chen, T. Cheng et al., "PubChem in 2021: new data content and improved web interfaces," *Nucleic Acids Research*, vol. 49, no. 1, pp. D1388–D1395, 2021.

[15] A. Daina, O. Michielin, and V. Zoete, "SwissTargetPrediction: updated data and new features for efficient prediction of protein targets of small molecules," *Nucleic Acids Research*, vol. 47, no. 1, pp. W357–W364, 2019.

[16] K. Gallo, A. Goede, R. Preissner, and B.-O. Gohlke, "SuperPred 3.0: drug classification and target prediction—a machine learning approach," *Nucleic Acids Research*, vol. 50, no. 1, pp. W726–W731, 2022.

[17] Z. Jin, H. Zhao, Y. Luo et al., "Identification of core genes associated with the anti-atherosclerotic effects of salvianolic acid B and immune cell infiltration characteristics using bioinformatics analysis," *BMC Complement Med Ther*, vol. 22, no. 1, p. 190, 2022.

[18] T. Barrett, S. E. Wilhite, P. Ledoux et al., "NCBI GEO: archive for functional genomics data sets—update," *Nucleic Acids Research*, vol. 41, no. 1, pp. D991–D995, 2012.

[19] D. Szklarczyk, R. Kirsch, M. Koutrouli et al., "The STRING database in 2023: protein–protein association networks and functional enrichment analyses for any sequenced genome of interest," *Nucleic Acids Research*, vol. 51, no. 1, pp. D638–D646, 2023.

[20] S. Zhu, H. Chen, X. Zhu et al., "Correlation network analysis provides important modules and pathways for human hyperlipidemia," *Critical Reviews in Eukaryotic Gene Expression*, vol. 29, no. 5, pp. 437–448, 2019.

[21] N. Dixit, H. Motwani, S. K. Patel, R. M. Rawal, and H. A. Solanki, "Decoding the mechanism of andrographolide to combat hepatocellular carcinoma: a network pharmacology integrated molecular docking and dynamics approach," *Journal of Biomolecular Structure and Dynamics*, pp. 1–19, 2023.

[22] Q. He, C. Liu, X. Wang et al., "Exploring the mechanism of curcumin in the treatment of colon cancer based on network pharmacology and molecular docking," *Frontiers in Pharmacology*, vol. 14, Article ID 1102581, 2023.

[23] P. Liu, S. Yang, Z. Wang, H. Dai, and C. Wang, "Feasibility and mechanism analysis of shenfu injection in the treatment of idiopathic pulmonary fibrosis," *Frontiers in Pharmacology*, vol. 12, Article ID 670146, 2021.

[24] S. K. Burley, C. Bhikadiya, C. Bi et al., "RCSB protein Data Bank: powerful new tools for exploring 3D structures of biological macromolecules for basic and applied research and education in fundamental biology, biomedicine, biotechnology, bioengineering and energy sciences," *Nucleic Acids Research*, vol. 49, no. D1, pp. D437–D451, 2021.

[25] R. M. Golsteyn, "Cdk1 and Cdk2 complexes (cyclin dependent kinases) in apoptosis: a role beyond the cell cycle," *Cancer Letters*, vol. 217, no. 2, pp. 129–138, 2005.

[26] A. Kwak, J. Lee, S. Lee et al., "Echinatin induces reactive oxygen species-mediated apoptosis via JNK/P38 MAPK signaling pathway in colorectal cancer cells," *Phytotherapy Research*, vol. 37, no. 2, pp. 563–577, 2023.

[27] Q. Lu, H. Huang, X. Wang et al., "Echinatin inhibits the growth and metastasis of human osteosarcoma cells through Wnt/β-catenin and p38 signaling pathways," *Pharmacological Research*, vol. 191, Article ID 106760, 2023.

[28] M. Kunnummal, M. Angelin, and A. V. Das, "PIWI proteins and piRNAs in cervical cancer: a propitious dart in cancer stem cell-targeted therapy," *Human Cell*, vol. 34, no. 6, pp. 1629–1641, 2021.

[29] G. I. Evan and K. H. Vousden, "Proliferation, cell cycle and apoptosis in cancer," *Nature*, vol. 411, no. 6835, pp. 342–348, 2001.

[30] M. Malumbres and M. Barbacid, "Cell cycle, CDKs and cancer: a changing paradigm," *Nature Reviews Cancer*, vol. 9, no. 3, pp. 153–166, 2009.

[31] Y. Ma, Q. Zhu, J. Liang et al., "A CRISPR knockout negative screen reveals synergy between CDKs inhibitor and metformin in the treatment of human cancer in vitro and in vivo,"

Signal Transduction and Targeted Therapy, vol. 5, no. 1, p. 152, 2020.

[32] M. Bury, B. Le Calvé, G. Ferbeyre, V. Blank, and F. Lessard, "New insights into CDK regulators: novel opportunities for cancer therapy," *Trends in Cell Biology*, vol. 31, no. 5, pp. 331–344, 2021.

[33] C. Chu, Y. Geng, Y. Zhou, and P. Sicinski, "Cyclin E in normal physiology and disease states," *Trends in Cell Biology*, vol. 31, no. 9, pp. 732–746, 2021.

[34] Y. Yang, C. Yang, T. Li et al., "The deubiquitinase USP38 promotes NHEJ repair through regulation of HDAC1 activity and regulates cancer cell response to genotoxic insults," *Cancer Research*, vol. 80, no. 4, pp. 719–731, 2020.

[35] A. Ali, J. Shafarin, H. Unnikannan et al., "Co-targeting BET bromodomain BRD4 and RAC1 suppresses growth, stemness and tumorigenesis by disrupting the c-MYC-g9a-FTH1axis and downregulation of HDAC1 in molecular subtypes of breast cancer," *International Journal of Biological Sciences*, vol. 17, no. 15, pp. 4474–4492, 2021.

[36] N. Stojanovic, Z. Hassan, M. Wirth et al., "HDAC1 and HDAC2 integrate the expression of P53 mutants in pancreatic cancer," *Oncogene*, vol. 36, no. 13, pp. 1804–1815, 2017.

[37] J. P. Smalley, I. M. Baker, W. A. Pytel et al., "Optimization of class I histone deacetylase PROTACs reveals that HDAC1/2 degradation is critical to induce apoptosis and cell arrest in cancer cells," *Journal of Medicinal Chemistry*, vol. 65, no. 7, pp. 5642–5659, 2022.

[38] J. Bartek and J. Lukas, "Chk1 and Chk2 kinases in checkpoint control and cancer," *Cancer Cell*, vol. 3, no. 5, pp. 421–429, 2003.

[39] H. Gali-Muhtasib, D. Kuester, C. Mawrin et al., "Thymoquinone triggers inactivation of the stress response pathway sensor CHEK1 and contributes to apoptosis in colorectal cancer cells," *Cancer Research*, vol. 68, no. 14, pp. 5609–5618, 2008.

[40] A. O. Fadaka, O. O. Bakare, N. R. S. Sibuyi, and A. Klein, "Gene expression alterations and molecular analysis of CHEK1 in solid tumors," *Cancers*, vol. 12, no. 3, p. 662, 2020.